Model Predictive Control: A Review of Its Applications in Power Electronics

Sergio Vazquez, Jose I. Leon, Leopoldo G. Franquelo, Jose Rodriguez, Hector A. Young, Abraham Marquez and Pericle Zanchetta

***Abstract*— Model predictive control (MPC) for power converters and drives is a control technique that has gained attention into the research community. The main reason is that although MPC presents high computational burden it can handle multivariable case and system constrains and nonlinearities easily in a very intuitive way. Taking advantage of that, MPC has been successfully used for different applications such as active front end, power converters connected to RL loads, uninterruptible power supplies and high performance drive for induction machines among others. This paper provides a review of the application of MPC in the power electronics area.**

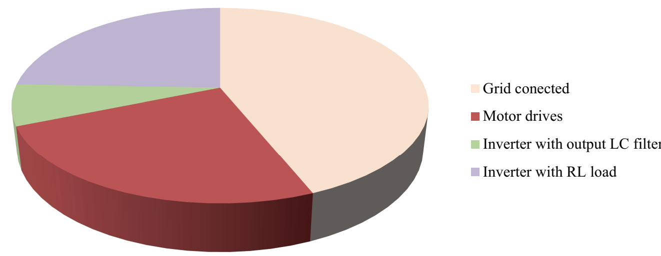

Fig. 1. Research works of MPC for PWM power converters published in IEEE conferences and journals from 2007 to 2012: Distribution regarding applications.

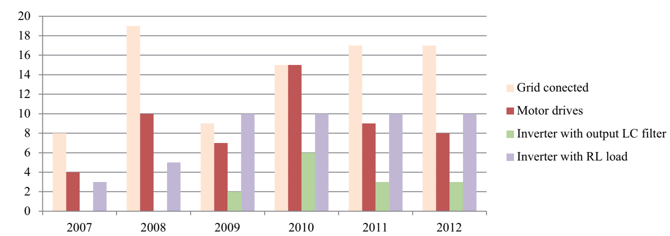

Fig. 2. Research works of MPC for PWM power converters published in IEEE conferences and journals from 2007 to 2012: Distribution regarding applications and year of publication.

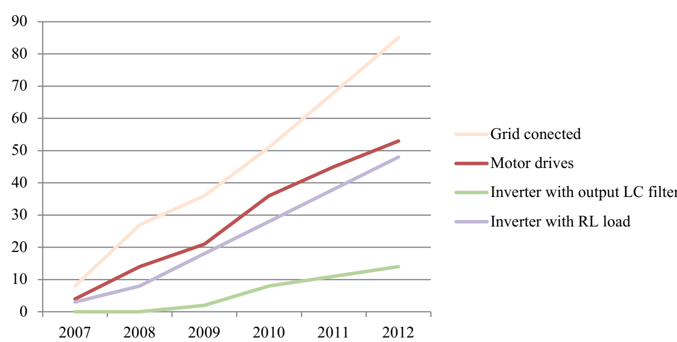

Fig. 3. Research works of MPC for PWM power converters published in IEEE conferences and journals from 2007 to 2012: Cumulative analysis for each application category.

I. Introduction

MODEL-BASED predictive control (MPC) presents a dramatic advance in the theory of modern automatic control [1]. Originally, MPC was studied and applied in the process industry, where it has been in use for decades [2]. Now, predictive control is being considered in other areas, such as power electronics and drives [3]–[6]. The reason for the growing interest in the use of MPC in this field is the existence of very good mathematical models to predict the behavior of the variables under control in electrical and mechanical systems. In addition, today's powerful microprocessors can perform the large amount of calculations needed in MPC at high speed and reduced cost.

The analysis of the research works published in the period form 2007 to 2012 in IEEE xplorer ® performing a search using the keywords "predictive" and "power converters" generate more than 200 papers of MPC applied to PWM power converters published in conferences and journals [7]. The applications covered by these research works can be categorized in four main groups: Grid connected converters, inverters with RL output load, inverters with output LC filters and high performance drives. Fig. 1 shows how these research works are distributed among these four groups. It is also interesting to study how these categories have attracted the attention of the research community along the last years. Fig. 2 and Fig. 3 present information about this issue. Fig. 2 shows that grid connected converters and high performance drives are the application where researchers have paid more attention being a current focus of interest. Fig. 3 addresses that research community attention has not decrease in this period and it is still increasing. It should be noticed the for all categories the cumulative line trends are positives.

S. Vazquez, J.I Leon, L.G. Franquelo and A. Marquez are with the Electronic Engineering Department, Universidad de Sevilla (Spain), (e-mail: sergi@us.es).

This paper presents the use of MPC for the four main categories of applications for PWM power converters that can be found in the literature. This includes a variety of applications like: Grid connected converters; Inverters with RL output load, Inverters with output LC filters and High performance drives. Basic issues of well established MPC algorithms are presented for these applications and new challenges for MPC control for power converters and drives are also addressed.

II. The MPC control strategy

Predictive control is understood as a wide class of controllers which main characteristic is the use of the model of the system for the prediction of the future behavior of the controlled variables over a prediction horizon N. This information is used by the MPC control strategy to provide the control action sequence for the system by optimizing a user defined cost function [8]. It should be noticed that the algorithm is executed again every sampling period and only the first value of the optimal sequence is applied to the system at instant k. The cost function can have any form but usually it is defined as

$$g = \sum_i \lambda_i \left(x_i^* - x_i^p\right)^2 . \quad (1)$$

Where x_i^* is the reference command and x_i^p the predicted value for variable x_i, λ_i is a weighting factor and index i stands for the number of variables to be controlled. In this simple way it is possible to include several control objectives (multivariable case), constrains and nonlinearities. The predicted values x_i^p are calculated by means of the model of the system to be controlled.

A. *MPC for power converters*

Application of MPC for power converters has increased due to the improvement of digital microcontrollers [3], [9]. This control technique requires a non negligible amount of calculations during small sampling times when applied for controlling power converters and drives.

There are several approaches to face the computational burden problem. In some cases, it is possible to solve the optimization problem offline by multi-parametric programming, thus the implementation is reduced to some calculations and a look-up-table [10]. Another way consists of using predictive techniques as generalized predictive control (GPC). GPC provides an online solution to the optimization problem and can be used for long prediction horizons without increasing significantly the computational cost [8], [11]. It should be noticed that GPC does not take into account switching of power semiconductors when it is applied for power electronics and drives. Therefore GPC only gives an exact solution to an approximated optimization problem. This approach can be followed when an explicit solution to the problem can be found. Usually this requires an unconstrained problem, but it calculates the output voltage reference to the inverter. This voltage should be generated by a PWM-SVM modulator. Thus GPC technique can take advantage of well established knowledge about PWM-SVM to optimize some aspects of the power converter systems [12].

Finally, the discrete nature of power converters can be considered for implementing MPC control strategies. In this way, finding the solution to the optimization problem can be reduced to evaluate the cost function only for the prediction of the system behavior for the power converter possible switching states. As a finite number of control actions are evaluated, this approach is called finite control set MPC (FCS-MPC). This technique has been extensively used for power converters due to the finite number of switching states they present [6].

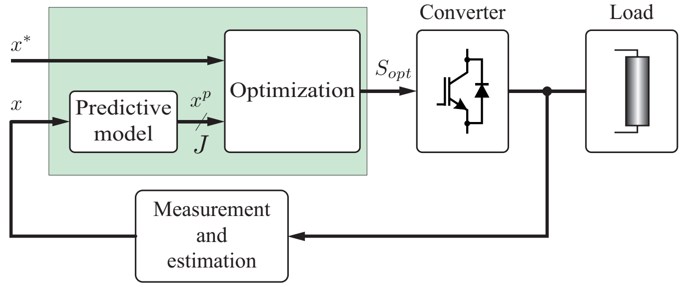

Fig. 4. FCS-MPC block diagram.

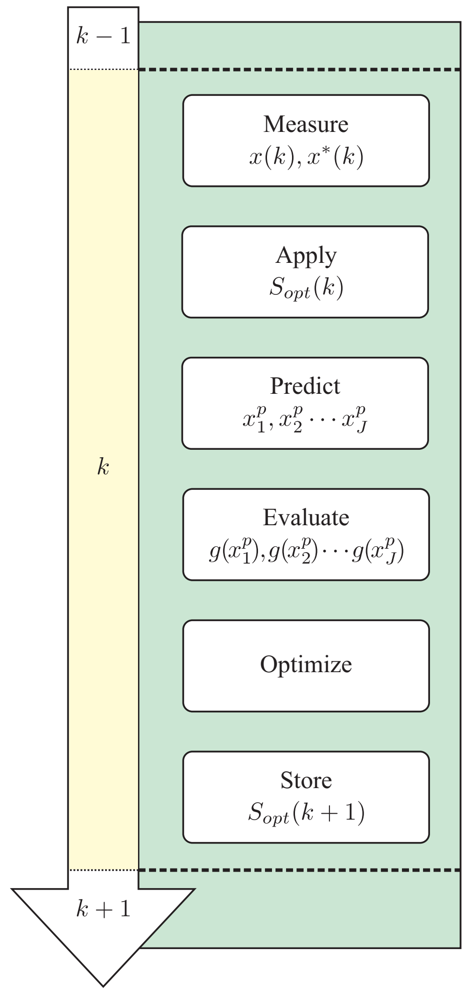

Fig. 5. Time diagram of the execution of the FS-MPC algorithm.

B. *FCS-MPC control principle*

Fig. 4 shows the block diagram of FCS-MPC, where a generic converter is used to feed a generic load. The converter presents J different switching states. The control objective pursuits that variable x has to follow the reference x^*. The FCS-MPC algorithm has the following basic steps:

1) Measure and/or estimate the controlled variables.

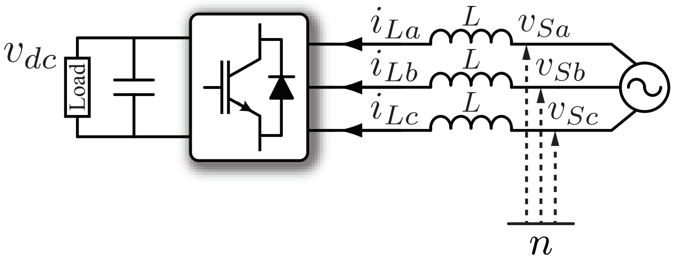

Fig. 6. Power circuit of the AFE.

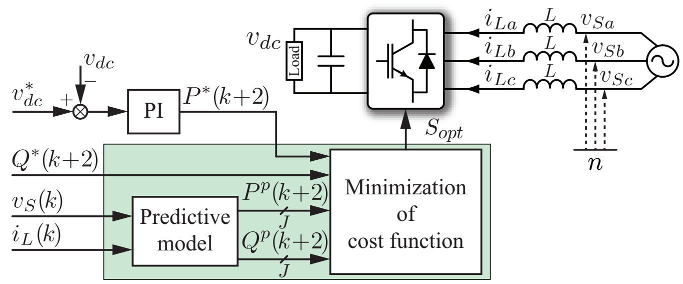

Fig. 7. Block diagram of the FCS-MPC control strategy for the AFE.

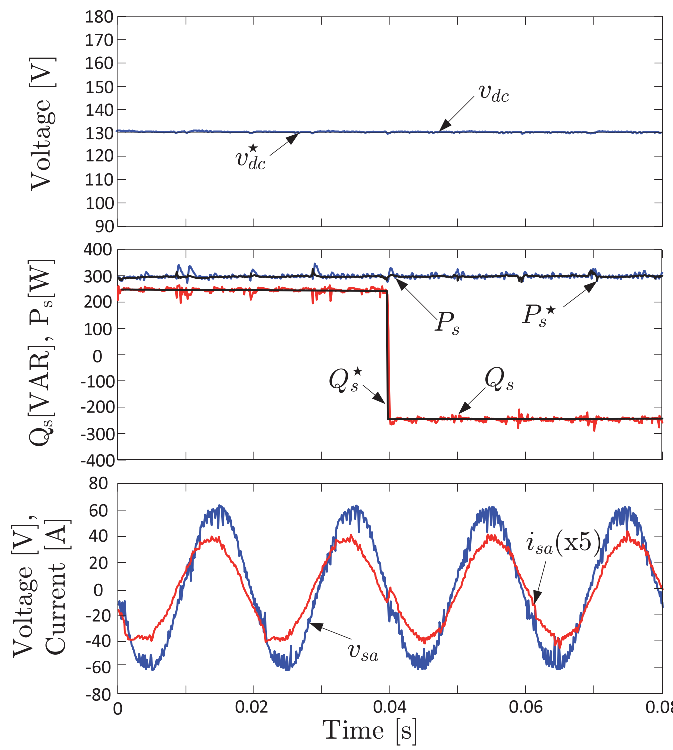

Fig. 8. Experimental results of the FCS-MPC-DPC for a three-phase two-level AFE.

2) Apply the optimal switching state (computed in the previous sampling period).
3) For every switching state of the converter, predict (using the mathematical model) the behavior of variable x in the next sampling interval x^p.
4) Evaluate the cost function, or error, for each prediction as, for instance: $g = |x^* - x^p|$
5) Select the switching state that minimizes the cost function, S_{opt} and store it for being applied to the converter at the next sampling period.

As discussed in [13] it is convenient to perform the prediction two time steps ahead, in order to reduce the effects of the delay introduced by the implementation of FCS-MPC in a digital platform. Another possibility to avoid the effect of the computation delay is to use a control strategy that only requires a small computation time. In this way, the optimal switching state is applied to the converter with this small delay, and before the following sampling instant [14]. A time diagram of the execution of the FCS-MPC algorithm is presented in Fig.5.

III. MPC FOR GRID CONNECTED CONVERTERS

Several applications use grid connected converters as one of their main components. This application includes active front end (AFE) for high performance drives, rectifiers, grid integration of renewable energies like wind or PV, energy storage systems, and are also used in FACTS devices as STATCOM, active power filter, or as a part of an UPFC or UPQC [15]–[17].

A. Control of an Active Front End

The power circuit of a grid connected converter through a smoothing inductor L is presented in Fig. 6. As shown, the main system variables are the grid current $i_{L,abc}$, grid voltage $v_{S,abc}$ and the output capacitor dc-link voltage v_{dc}. The load connected to the dc-link represents any generic load connected to an AFE. Thus it can be a resistor for a rectifier, a PV panel or a converter to control the torque and/or speed of a wind turbine for grid integration of renewable energies, etc.

The main objective of the control strategy is to calculate the output inverter voltage $v_{I,abc}$ in order to regulate the output dc-link capacitor voltage to a reference v^*_{dc} for any connected load and inject into the grid any reactive power command reference q^*.

There are several alternatives for designing the control algorithm for an AFE. In general, a cascade control structure is used. An external control loop is employed to regulate the dc-link voltage. On the other hand an internal control loop is adopted to track the grid currents or the instantaneous active and reactive power references regarding the states variables used to develop this controller [18], [19].

MPC has been mainly used as control strategy for the inner control loop. Although some works developing grid current controllers can be found in the literature the main approach has been the direct power control (DPC) for tracking the commands for the instantaneous active and reactive powers, P and Q. Application of FCS-MPC-DPC and predictive DPC

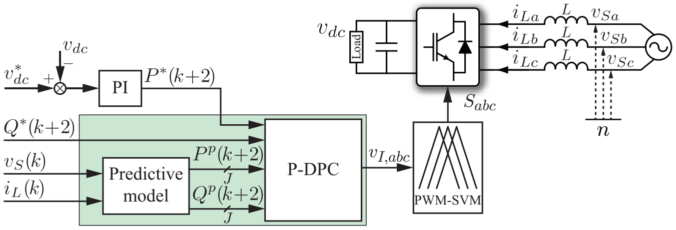

Fig. 9. Block diagram of the P-DPC control strategy for the AFE.

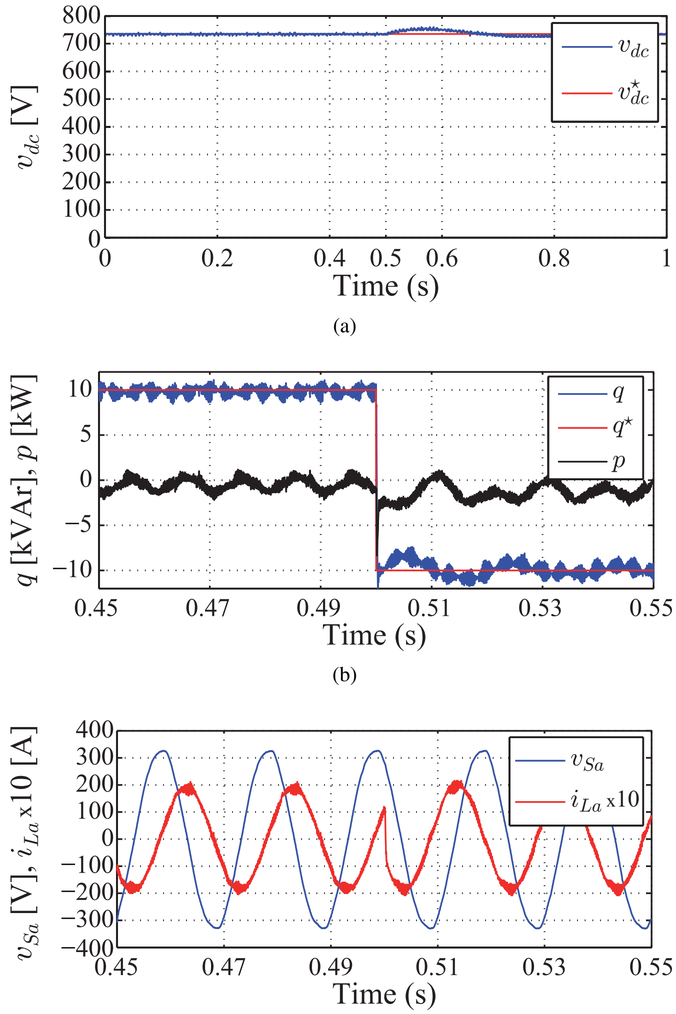

Fig. 10. Experimental results of the P-DPC for a three-phase two-level AFE for a reactive power command step from 10 to -10 kVAr. (a) dc-link voltage; (b) Instantaneous active and reactive power; (c) Grid voltage and output current for phase a.

with SVM modulation strategy (P-DPC) can be considered as well established [14], [20]–[22].

The block diagram of the FCS-MPC-DPC strategy is presented in Fig. 7. In this case, the model of the system is used to predict values of the instantaneous active and reactive power over a prediction horizon $N = 1$, $P^p(k+2)$, $Q^p(k+2)$. In [14], [20] a three-phase two-level AFE was controlled adopting this strategy. The algorithm was developed in the $\alpha\beta$ frame. Therefore, only the seven possible output vectors were considered to perform the prediction, thus the number of switching states is $J = 7$. Once the seven output voltage predictions are calculated the cost function

$$g = (P^*(k+2) - P^p(k+2))^2 + (Q^*(k+2) - Q^p(k+2))^2 \quad (2)$$

is minimized in order to find the inverter output vector that should be applied in the next sampling period.

Fig. 8 presents experimental results obtained using this strategy [14]. It should be noticed that predictions in instants $(k+2)$ are used in order to compensate for the control action delay of the digital implementation of the control strategy.

Another way to perform the predictive controller for the AFE is the P-DPC. The block diagram of the P-DPC strategy is presented in Fig. 9. Like GPC, P-DPC strategy does not take into account switching of power semiconductors therefore it just provides an exact solution to an approximated optimization problem. Besides, P-DPC considers an unconstrained MPC problem. Thus an explicit solution can be obtained providing the control action to be applied once the cost function (2) is minimized. Therefore, an optimal switching vector sequence can be calculated. The control strategy provides the switching vectors and the switching times thus a PWM-SVM modulation strategy is necessary to generate the firing pulses.

Compared with FCS-MPC, the P-DPC algorithm uses an external modulator thus constant switching frequency is obtained. This can be considered as an advantage specially in the AFE application because for grid connected converters exist high demanding codes that impose strict limits to the low order harmonics that can be injected into the grid. FCS-MPC presents variable switching frequency thus grid current has a widespread harmonic spectrum. On the other hand P-DPC provides constant switching frequency thus grid current harmonic spectrum is concentrated around the switching frequency decreasing the cost of the output L filter. Fig. 10 shows experimental results obtained using the P-DPC strategy for a STATCOM application when an instantaneous reactive power command step is imposed [22].

It should be noticed that the outer control loop to regulate the dc-link capacitor voltage is usually solved using a conventional PI controller. However, there exist some solutions that replace the PI control for a MPC strategy [14].

B. Control of an Active Filter

In its classical configuration, an active power filter (APF) basically consists of a voltage source inverter (VSI) whose dc side is connected to a capacitors bank whereas its ac side is connected to the mains through a suited filter, usually formed by a set of series inductors as shown in Fig. 11 (referring to the most common 3-wires configuration without neutral). In such configuration, ideally the APF is able to operate as a controllable current generator, drawing from the mains any set of current waveforms having a null sum. Therefore, an APF is ideally able to compensate the unbalanced, reactive and harmonic components of the currents drawn by any load, in such a way that the global equivalent load, as seen from the grid, resembles a resistive balanced load drawing about the

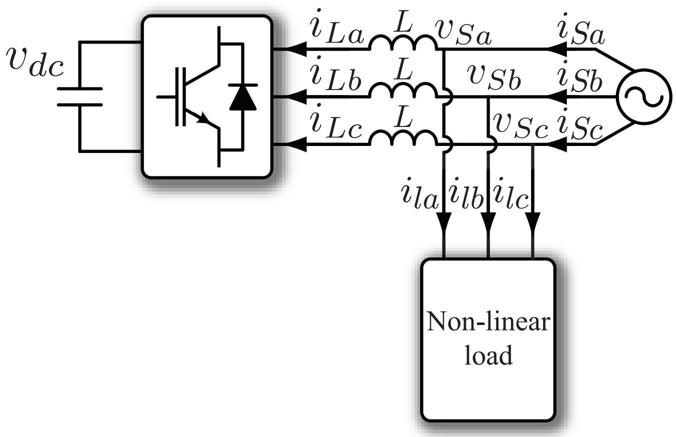

Fig. 11. Power circuit of a 3-wires APF.

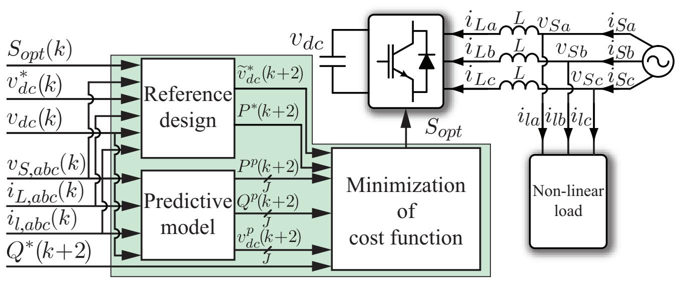

Fig. 12. Block diagram of the FCS-MPC control strategy for the APF.

same active power. In fact, since under steady-state conditions the voltage of the dc bus is intended to remain about constant and close to the design level to permit an indefinitely long operation then in practice the currents drawn by the APF must give rise to a small net average power flow to exactly balance its internal losses.

The active filter modeling procedure and the reference quantities calculations are reported in [23], while the control block scheme is shown in Fig. 12. The MPC uses the prediction model and the reference derivation to select the switching functions $S(k+1)$ which minimize a cost function as:

$$\begin{aligned} g &= \frac{\lambda_1}{v_{dcR}}\left(\widetilde{v}^*_{dc}(k+2) - v^p_{dc}(k+2)\right)^2 \\ &+ \frac{\lambda_2}{P_{SR}}\left(P^*_S(k+2) - P^p_S(k+2)\right)^2 \\ &+ \frac{\lambda_3}{P_{SR}}\left(Q^*_S(k+2) - Q^p_S(k+2)\right)^2 \end{aligned} \quad (3)$$

Where v^*_{dc}, P^*_S and Q^*_S are the reference values of dc-link voltage, active and reactive power respectively; v^p_{dc}, P^p_S and Q^p_S are predicted values of dc-link voltage, active and reactive power respectively; P_{SR}, and v_{dcR} are respectively

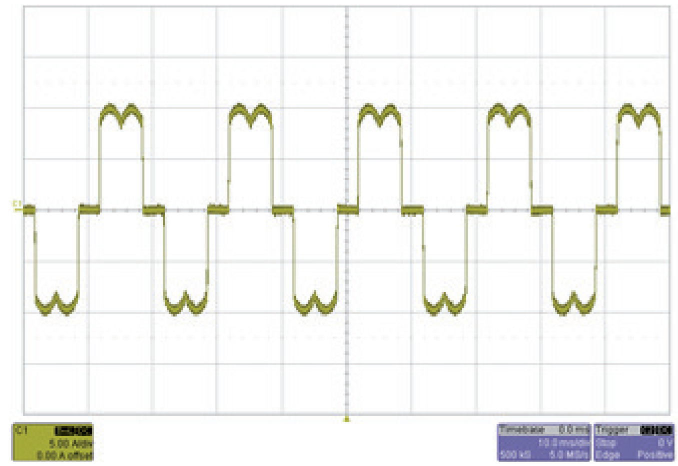

(a)

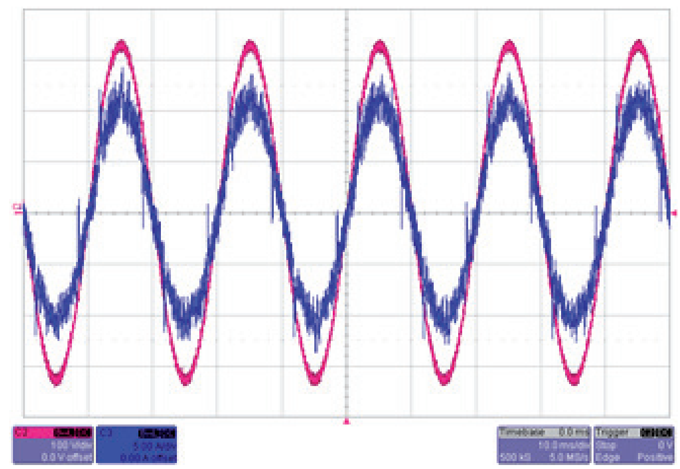

(b)

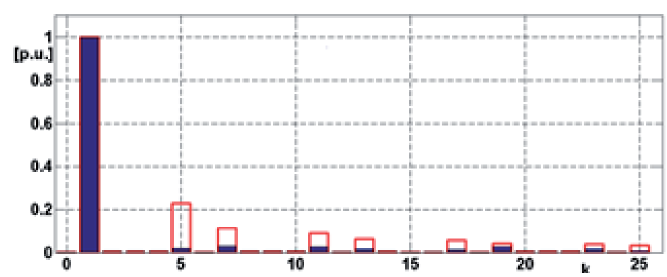

(c)

Fig. 13. Experimental results of the FCS-MPC for a 3-wired three-phase two-level APF. (a) Supply current before compensation; (b) Supply current after compensation and supply voltage. (c) Spectrum of currents in (a) and (b).

rated values of active power and dc link voltage, λ_1, λ_2 and λ_3 are weighting factors that allow a proper balance among deviations in voltage, active and reactive power, $\widetilde{v}^*_{dc}(k+2)$ represents a filtered voltage reference with a certain prediction horizon [23].

According to the scheme of Fig. 11, the APF experimental prototype chosen to verify the effectiveness of the FCS-MPC control includes a standard 3-leg IGBT based VSI inverter. The implemented control algorithm operates at fixed sampling frequency $f_s = 50$ kHz. To reproduce a distorted current in the grid, a non-linear load constituted by a 3-phase diode bridge rectifier supplying a resistor having a rated power $P_{SR} = 5$ kW was considered [23].

At full power the load draws the distorted current in Fig. 13a where the vertical axis measures 5A/div while the horizontal one 10ms/div; after APF compensation the mains currents waveform is shown in Fig. 13b (5A/div) together with the supply voltage (100V/div). The compensation action results in a unity power factor operation and quasi sinusoidal current with a superimposed high-frequency ripple due to inverter commutation and the nature of the FCS-MPC control action itself. The achieved benefits and therefore the effectiveness of the control action were also confirmed in spectral terms by comparing the mains current spectrum and the load current spectrum in Fig. 13c, resulting in a reduction of major low-order harmonics, which permits to achieve a THD$<$ 5% starting from a THD$>$ 29%, where the THD is calculated including up to the 50^{th} harmonic.

IV. MPC FOR INVERTERS WITH RL-LOAD

A. Control of a matrix converter

The direct matrix converter (DMC) is a type of static power converter in which the load is directly connected to the mains through a set of bidirectional switches. The power circuit of a DMC is shown in Fig. 14. This topology does not require a dc-link stage with energy storage as most power converters; this reduces the weight and size of the converter, making it suitable for applications that require high power density, such as aerospace.

Control approaches based on FCS-MPC have been extensively tested for the DMC [24], [25], showing the effectiveness and relative simplicity of the predictive methods over the traditional ones such as space-vector modulation [26]. The block diagram of the predictive control of load current and input power factor is presented in Fig. 15. The predictive controller relies on mathematical models for the prediction of both the input reactive power and the output current. Each prediction block depicted in Fig. 15 yields 27 predictions for the controlled variables, one for each of the different valid switching states of the DMC. A further stage of the algorithm then minimizes a cost function in order to determine the optimal combination of gating signals to be applied to the converter at the next sampling period.

The cost function for the simultaneous control of input reactive power Q and output current i_o is the following:

$$g = |i_o^* - i_o^p| + \lambda \, |Q^* - Q^p| \,, \tag{4}$$

where i_o^*, Q^*, i_o^p and Q^p are the reference and the predicted values of the output current and the input reactive power, respectively; λ is a weighting factor used to adjust the relative importance of both control objectives within the cost function.

Results of the predictive control of the DMC are shown in Fig. 16. The output current tracks its reference accurately, as can be seen in Fig. 16a. The input reactive power is controlled starting from time $t = 0.4\,[\mathrm{s}]$, in Fig. 16c. It can be observed that from that instant on, after a short transient, the input current becomes sinusoidal and in phase with the line voltage.

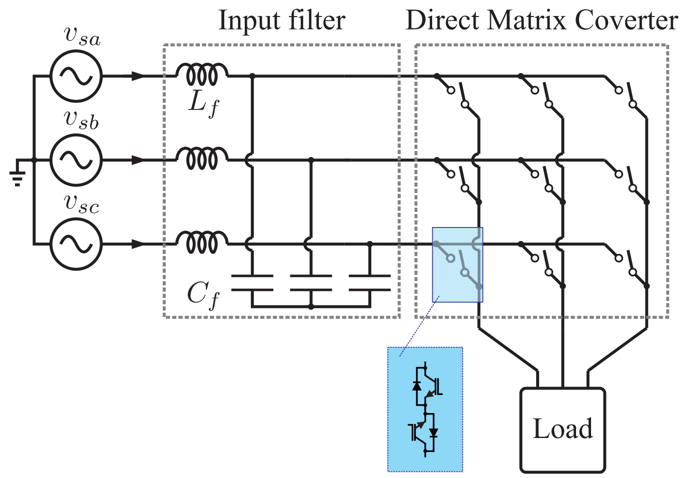

Fig. 14. Power circuit of a three-phase direct matrix converter.

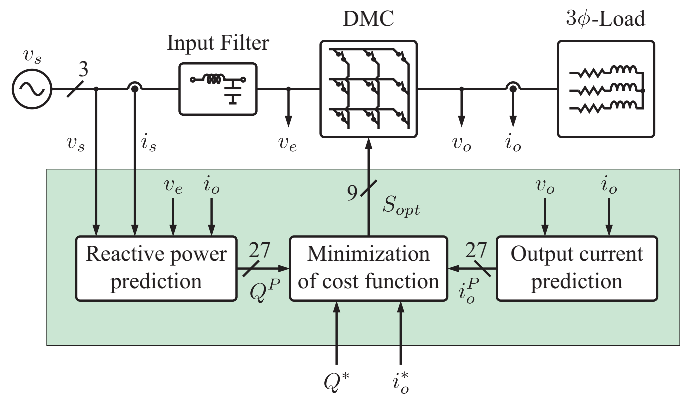

Fig. 15. Block diagram of the predictive current and reactive power control of a direct matrix converter.

B. SHE and SHM for power converters

1) Selective harmonic elimination technique: The selective harmonic elimination (SHE) strategy is specially well suited for high-power applications where the power losses must be kept below strict limits. The well-known SHE technique is based on offline calculations and the generation of a pre-programmed voltage waveforms with very low number of commutations and eliminating some low order harmonics [27]. Using the predictive control to implement the SHE method, the MPC-SHE control objective is to follow the voltage reference, to eliminate low order harmonics and to reduce switching losses [28]. These three objectives are included in the cost function

$$\begin{aligned} g =& SDFT_{f1}\left\{|\mathbf{v}_s^* - \mathbf{v}_s^p|\right\} && (5)\\ &+ \lambda_f \sum_{i}^{M} SDFT_{fi}\left\{|\mathbf{v}_s^* - \mathbf{v}_s^p|\right\} && (6)\\ &+ \lambda_{sw} x_{sw}^p, && (7)\\ &i = 0, 2, 3, 4, \ldots, M. \end{aligned}$$

In this cost function, the sliding discrete fourier transform (SDFT) is used. The SDFT is a recursive implementation of

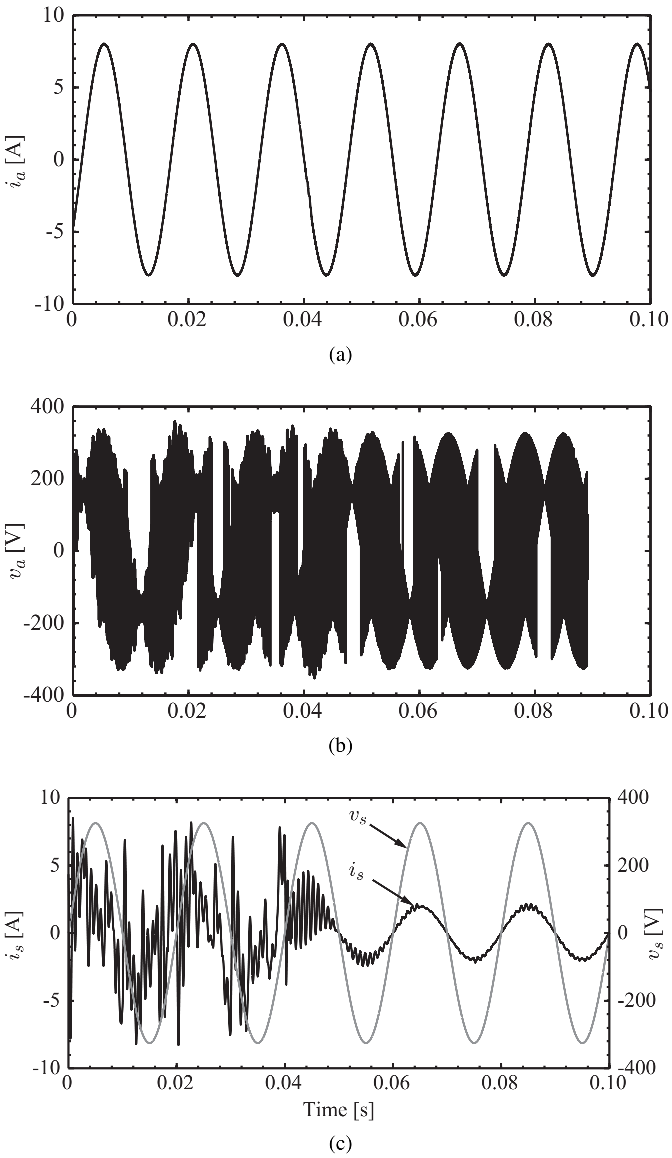

Fig. 16. Predictive current control of a direct matrix converter. (a) Output current. (b) Output voltage. (c) Input current and grid voltage (phase a).

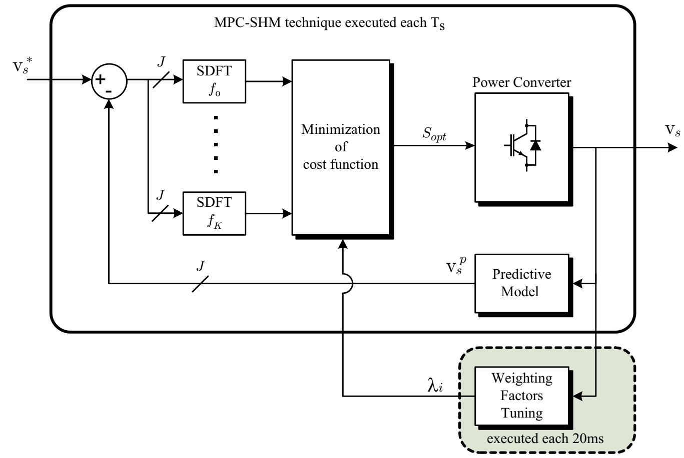

Fig. 17. Block diagram of the proposed MPC-SHM technique.

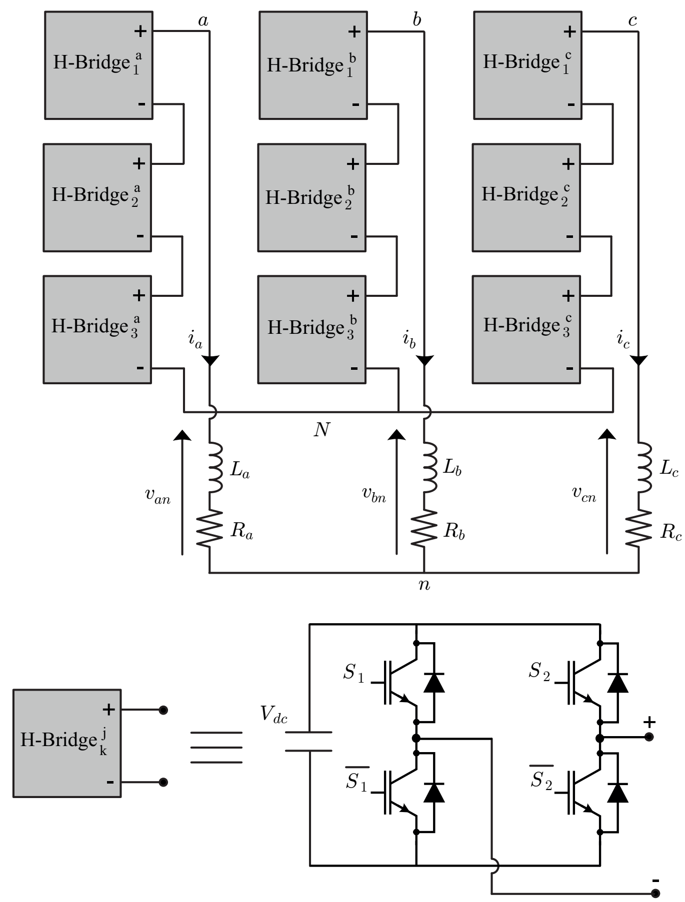

Fig. 18. Power circuit of a H-bridge multilevel converter (three H-bridges per phase) connected to a RL load.

the discrete Fourier Transform algorithm used to calculate a finite number of single frequency spectral components with very low computational cost [29].

The first term (5) evaluates the error between the reference and the predicted output voltage vector tuned to the fundamental frequency f_1.

The second term (6) is the sum of all those frequencies (up to M^{th} order) that need to be eliminated. The weighting factor λ_f is used to control the importance of this term in the cost function, in this way the frequency elimination can be relaxed or strengthened in comparison to the fundamental frequency tracking, depending on design considerations.

Finally, the third term (7) is used to reduce the number of commutations introducing weighting factor λ_{sw} to keep the power losses below acceptable limits.

2) Selective harmonic mitigation technique: An evolution of SHE is the selective harmonic mitigation (SHM) technique which is based on pre-programmed waveforms non eliminating the low order harmonics but reducing the distortion below the limits imposed by a grid code [30], [31].

The control objective of the MPC-SHM is to follow the voltage reference, to control the harmonic distortion keeping it below the limits imposed in the grid code and to reduce the switching losses as much as possible [32]. These three objectives are included in a cost function which is similar to that introduced for the MPC-SHE method. In this case, the second term (6) has to be modified being the sum of

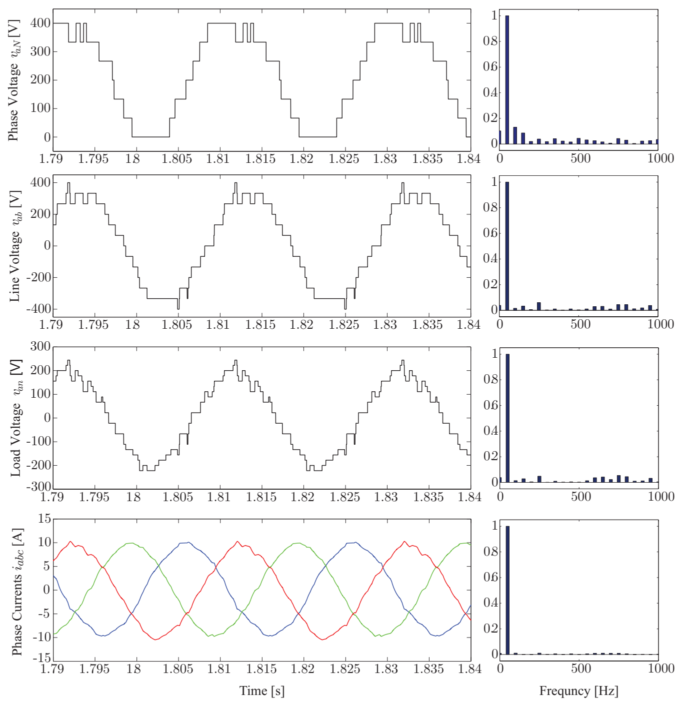

Fig. 19. Predictive harmonic mitigation phase output voltage v_{aN}, line voltage v_{ab}, load voltage v_{an} and load currents i_a,i_b,i_c for a 7-level CHB.

the distortion of those harmonics that have to be kept below acceptable limits imposed by the grid code from the 2^{nd} to the K^{th} harmonic. In fact, the mathematical expression of the MPC-SHM cost function is similar to the MPC-SHE one but considering harmonics up to K^{th} order where K is higher than M. Another difference between both cost functions is that a weighting factor λ_i is associated to each i^{th} order harmonic distortion that has to be reduced. This fact gives the chance to relax the condition of eliminating the distortion of those harmonics. The proposed MPC-SHM technique can be summarized using the block diagram represented in Fig. 17 where a weighting factors tuning block has been added to the previously introduced MPC-SHE method. For each harmonic, the weighting factors tuning block relaxes the weighting factor λ_i if the i^{th} harmonic distortion is below the limit of the grid code or make it higher in the opposite case. This dynamic weighting factors adjustment is made at fundamental frequency.

The MPC-SHM method has been tested in a three-phase cascaded H-bridge multilevel converter (three H-bridges per phase) connected to a RL load as depicted in Fig. 18. On the other hand, Fig. 19 shows the converter phase output voltage V_{aN}, the line-line voltage V_{ab}, the load voltage V_{an} and the load currents i_a, i_b and i_c. In addition, the respective harmonic spectra are shown next to each waveform. A deep analysis of the data shows that the distortion of harmonics considered in the cost function (up to harmonic 10^{th}) is always below the limit imposed. In addition, the average switching frequency of the MPC-SHM method is lower to that obtained with the MPC-SHE technique dealing with the same number of harmonics. This phenomenon appears because the SHM relaxes the conditions of the harmonic distortions compared with the SHE method and this fact makes easier to find better solutions leading to lower power losses.

C. Control of multilevel inverters

The FCS-MPC method has been applied to multilevel converters for multiple applications. Among the multilevel converter topologies, the neutral-point-clamped converter (NPC), the flying-capacitor converter (FC) and the cascaded H-bridge converter (CHB) are the ones with vast industrial success. These topologies are normally used for medium-voltage high-power applications at the expense of a large number of power semiconductors and more complex control and modulation algorithms. The FCS-MPC method for multilevel inverters has to take into account the usual control objectives present in other converter topologies and applications but extra control targets have to be included such as the balance of the floating dc voltages (if needed) and the reduction of the switching losses (required because for high-power applications the effective switching frequency and consequently the power losses have to be limited). Some examples are here addressed:

1) NPC inverter topology: The three-level NPC converter has the dc-link bus divided in two parts that should be balanced. So, this fact has to be included in the cost function. The dc voltage balance is achieved by the FCS-MPC method but at the expense of changing the switching state almost each sampling time. So, the result is not satisfactory because it leads to high switching losses. So, a limitation in the switching frequency has to be included in the cost function as well. Thus a possible cost function could be

$$g = \mid i_\alpha^* - i_\alpha^p \mid + \mid i_\beta^* - i_\beta^p \mid + \lambda_{dc} \mid v_{C1}^p - v_{C2}^p \mid + \lambda_n n_c. \quad (8)$$

In the cost function, the first term is focused on the current tracking which is the application of this FCS-MPC method. The second term is proportional to the absolute difference between the voltage predictions of both capacitors, so a switching state that generates smaller differences will be preferred leading to a voltage balance situation. Finally, the third term is proportional to the number of commutations to get to the next switching state n_c, so a switching state that implies fewer commutations of the power semiconductors will be preferred. The weighting factors λ_{dc} and λ_n handle the relation between terms dedicated to current reference tracking, voltage balance and reduction of switching frequency [33].

2) CHB inverter topology: The FCS-MPC method can be also applied to achieve current tracking control in a three-phase cascaded H-bridge converter with two H-bridges per phase [34]. In this case, the cost function only takes into account the current tracking:

$$g = \mid i_\alpha^* - i_\alpha^p \mid + \mid i_\beta^* - i_\beta^p \mid . \quad (9)$$

In the CHB inverter case, there are a high number of possible switching combinations (125 for this topology where the dc voltages of the H-bridges are fixed) so the computational cost of the FCS-MPC method can become excessively high. In [34], this is solved eliminating the redundant switching states with higher common-mode voltages. In addition, only the last

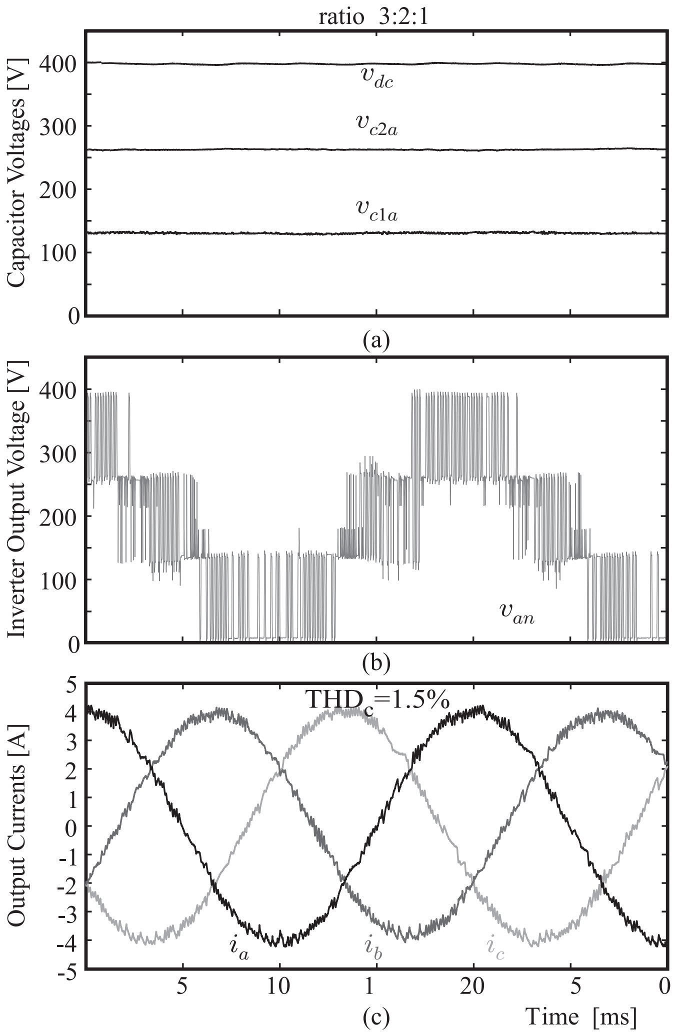

Fig. 20. Experimental results for the FCS-MPC applied to the FC with ratio 3:2:1: Capacitor voltages of phase a, inverter output voltage of phase a and output currents (taken from [35]).

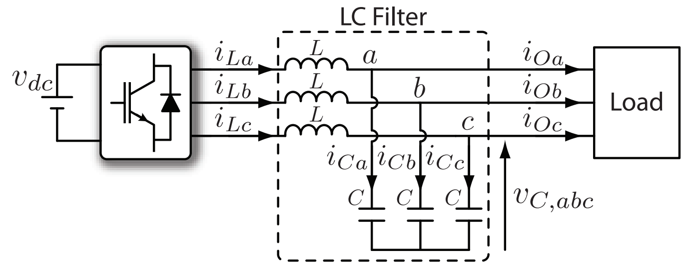

Fig. 21. Power circuit of a three-phase inverter with output LC filter.

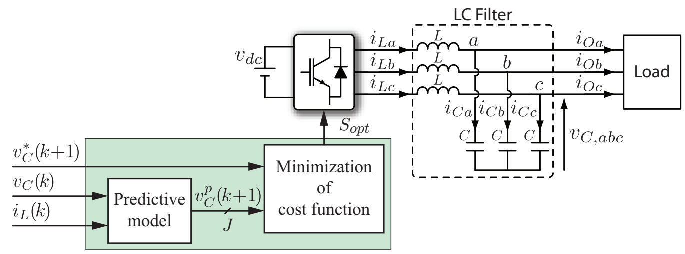

Fig. 22. Block diagram of the FCS-MPC control strategy for a three-phase inverter with output LC filter.

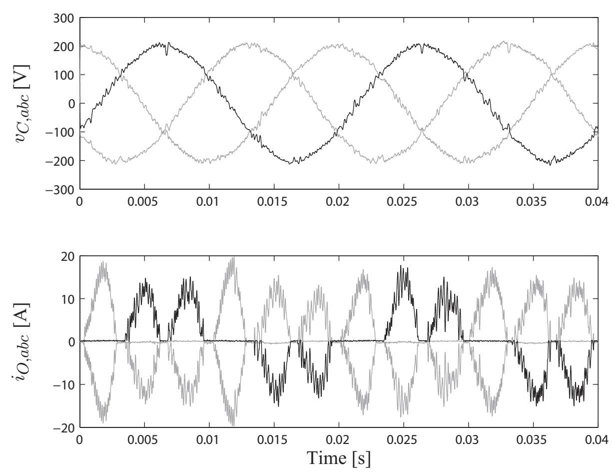

Fig. 23. Experimental results for the FCS-MPC: output voltages and currents in steady state for a non-linear load and a reference amplitude of 200V.

applied switching state and the six states surrounding it in the space vector diagram are taken into account. This fact reduces to seven the number of possible combinations leading to the same computational cost of a conventional three-phase two-level converter at the expense of solving a suboptimal problem and loosing dynamic response.

3) FC inverter topology: A similar FCS-MPC strategy can be applied to the FC converter. In [35], it is presented a cost function to achieve current tracking and floating voltages control of a three-phase FC converter with two floating capacitors per phase. In this case, the cost function includes the current tracking term and the floating voltages control term as follows:

$$g = g_a + g_b + g_c \tag{10}$$

where, g_a, g_b and g_c follow the next expression ($x \in a, b, c$)

$$g_x = (i_x^* - i_x^p)^2 + \lambda_{dc1}\left(v_{c1x}^* - v_{c1x}^p\right)^2 + \lambda_{dc2}\left(v_{c2x}^* - v_{c2x}^p\right)^2. \tag{11}$$

An interesting point to be highlighted is that, with the three-phase FC converter with two floating capacitors per phase, there are 512 possible switching combinations so the computational cost of the FCS-MPC method can become excessively high. In [35], this is solved ignoring the interaction through the load neutral point in the prediction step. This reduces the possible switching combinations to 24 leading to a high reduction in the computational cost at the expense of limiting a control degree.

In order to illustrate the good performance of FCS-MPC method for multilevel converters, the results for the FC inverter are represented in Fig. 20. As can be observed, the control objectives, current tracking and control of the floating voltages, are achieved.

V. MPC FOR INVERTERS WITH OUTPUT LC FILTER

Inverters with output LC filter are used when it is necessary to obtain a sinusoidal output voltage with very low harmonic content. This is the case of sensitive loads, or drives for

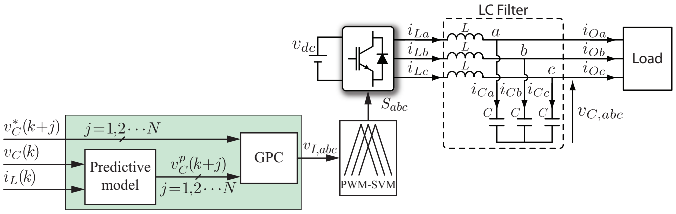

Fig. 24. Block diagram of the GPC control strategy for a three-phase inverter with output LC filter.

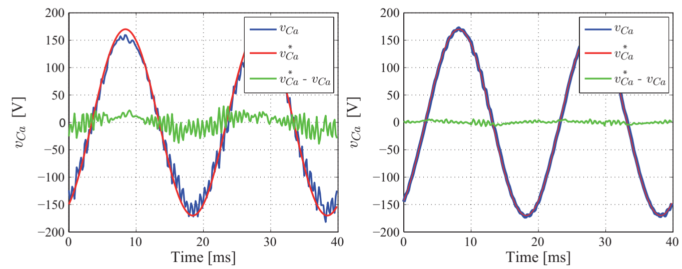

(a) (b)

Fig. 25. System performance for the GPC strategy for different values of N and λ: (a) Phase a voltage and its reference for $N = 5$ and $\lambda = 0.0$. (b) Phase a voltage and its reference for $N = 6$ and $\lambda = 1.05$.

machines in order to reduce the input voltage harmonics and increase its lifespan or avoid problems caused by high values of dv/dt. These inverters are also employed when a voltage source is needed like in FACTS devices as SSSC, DVR or as a part of an UPFC or UPQC. However, its most important application is as the main converter of uninterruptible power supply systems (UPS).

The power circuit of an inverter with output LC filter connected to a generic load is shown in Fig. 21. As shown, the main system variables are the output inductor current $i_{L,abc}$, output capacitor voltage $v_{C,abc}$, output capacitor current $i_{C,abc}$ and output load current $i_{O,abc}$. The main objective of the control strategy is to calculate the output inverter voltage $v_{I,abc}$ in order to track an output capacitor voltage reference $v^*_{C,abc}$ for any connected load.

There are several alternatives for designing the control algorithm for an inverter with output LC filter [36]. MPC is a very interesting option for this application, because high performance of the overall system can be achieved with a very simple algorithm. Application of FCS-MPC and GPC for an UPS system can also be found in the literature [12], [37].

The block diagram of the FCS-MPC strategy is presented in Fig. 22. In this case, the model of the system is used to predict the output capacitor voltage over a prediction horizon $N = 1$, $v^p_C(k+1)$. In [37] this strategy was adopted and the controller was developed for a three-phase two-level inverter in the $\alpha\beta$ frame. Therefore, only the seven possible output vectors were considered to perform the prediction, thus the number of switching states is $J = 7$. Once the seven output voltage predictions are calculated the cost function

$$g = \left(v^*_{C,\alpha} - v^p_{C,\alpha}\right)^2 + \left(v^*_{C,\beta} - v^p_{C,\beta}\right)^2 \qquad (12)$$

is minimized in order to find the inverter output vector that should be applied in the next sampling period.

Fig. 23 shows experimental results obtained using this strategy when a non linear load is connected to the inverter [37]. It should be noticed that $i_{O,abc}$ has been considered as a perturbation. In this way, $i_{O,abc}$ was not measured but a observer was used to enhance the performance of the system.

Prediction horizons N higher than 1 can provide in some cases better performance than using $N = 1$. This issue has been investigated for a UPS system using the FCS-MPC strategy [38]. The main problem is that computation burden increases exponentially with N. Therefore it is difficult the practical implementation of this approach.

Another way to increase the prediction horizon N is to use a GPC strategy to calculate the control action. The GPC uses a CARIMA model to predict the system variables with long prediction horizon values [11]. The block diagram of the GPC strategy is presented in Fig. 24. In this case, it is considered an unconstrained MPC problem. Thus an explicit solution can be obtained providing the control action to be applied once the cost function

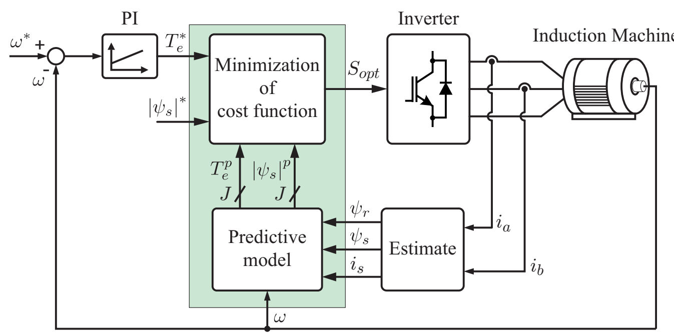

Fig. 26. Block diagram of the predictive torque control of an induction machine.

$$g = \sum_{j=1}^{N} \left\| v^*_{C,abc}(t+j) - v^p_{C,abc}(t+j) \right\|^2 - \lambda \Delta u(t)^2 \qquad (13)$$

is minimized.

Compared with FCS-MPC, the GPC algorithm requires an external modulator but this provides the benefit of presenting constant switching frequency making the design of the output LC filter easier. Fig. 25 shows experimental results obtained using the GPC strategy when a linear load is connected to the inverter for different values of N and λ [12]. It should be noticed that tuning correctly the prediction horizon N and the weighting factor λ can increase significantly the performance of the system.

VI. MPC FOR HIGH-PERFORMANCE DRIVES

For the control of high-performance drives there exist two well-established methods: field-oriented control (FOC) and

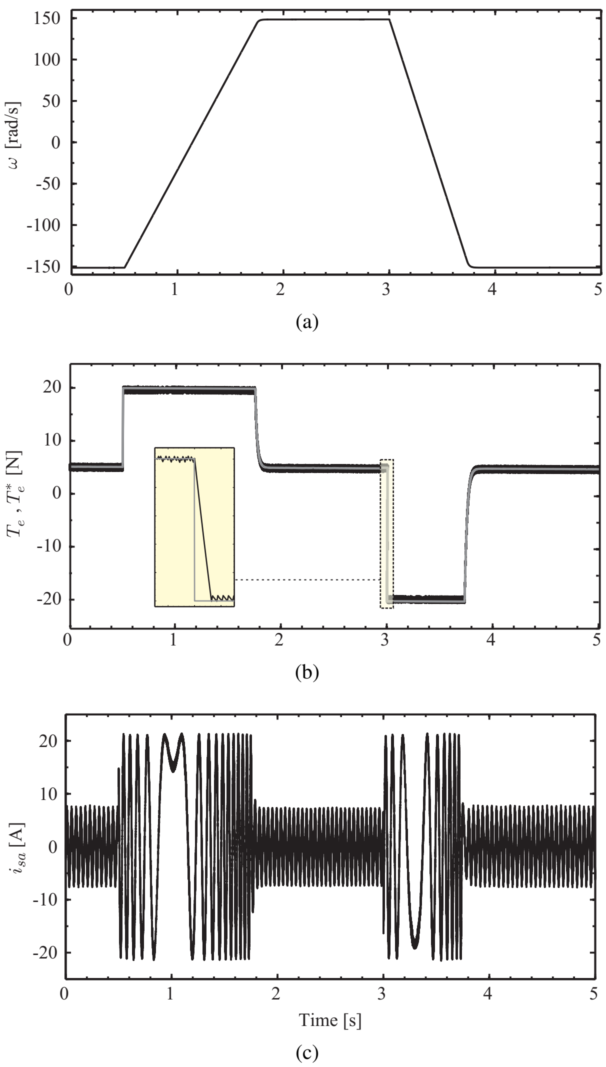

Fig. 27. Predictive torque control of an induction machine. (a) Angular speed. (b) Electrical torque. (c) Stator current (phase a).

direct torque control (DTC) [39]. The first one is able to perform a decoupled control of torque and flux by controlling separately the quadrature and direct components of the stator current in a rotating coordinate frame which is synchronous with the rotor flux.

On the other hand, the DTC approach is also able to perform an independent control of torque and flux, by employing non-linear hysteresis controllers and a logic based on a look-up table in order to select the appropriate switching states of the converter.

A third alternative, predictive torque control (PTC), has been proposed recently [40]. In the PTC algorithm, a cost function that gathers the tracking error of torque and stator flux magnitude is employed:

$$g = |T_e^* - T_e^p| + \lambda \left| |\psi_s|^* - |\psi_s|^p \right|, \qquad (14)$$

where T_e^*, $|\psi_s|^*$, T_e^p and $|\psi_s|^p$ are the reference and predicted values of electrical torque and the magnitude of the stator flux, respectively. The parameter λ is a weighting factor that allows giving more or less relevance to each of the control objectives. Following the operation principle of FCS-MPC, the switching state applied to the converter at each sampling period corresponds to the one that minimizes the cost function. The block diagram of PTC is presented in Fig. 26. An estimator is required in order to compute the stator and rotor fluxes. Then, a mathematical model is used to predict the future behavior of the torque and stator flux using the flux estimations and the measurements of stator current and mechanical angular speed of the machine. In [40] this technique was used together with three-phase two-level inverter. In this way, the number of switching states is $J = 7$. Therefore, the predictions associated to the seven different voltage vectors are evaluated in an optimization stage in order to select the optimum switching state S to be applied to the inverter. For the generation of the electrical torque reference, an external control loop with a PI controller was used.

Results of the PTC of an induction machine are shown in Fig. 27. The speed control is presented in Fig. 27a, where reference step changes from -150 to $150\,[\mathrm{rad/s}]$ and from 150 to $-150\,[\mathrm{rad/s}]$ are applied at times $t = 0.5$ and $t = 3.0\,[\mathrm{s}]$, respectively. The dynamic performance of the torque tracking can be observed in Fig. 27b, where it is clear that PTC provides a very fast response. The stator current for phase a is plotted in Fig. 27c, showing a sinusoidal waveform, despite no current controllers are directly implemented.

VII. Past, present and future challenges of MPC for power converters and drives

MPC has been used as a good solution for industrial applications since decades [5], [41]. However, once the simplicity and the good performance of the MPC controller in the power electronics field has been demonstrated, the question to be solved is why it is not already extensively used in the industry.

As a major challenge, the MPC needs an accurate model of the system and this is not usually a simple task in highly dynamic systems. However, in the last years the modeling of complex electrical systems has been greatly improved and this challenge can be solved. Although still is necessary more research, now it is possible to find applications of MPC to power converters where Luenberger and extended state observers are used to avoid the effects of systems parameters uncertainties [37], [42], [43].

A drawback of the MPC strategies is the exponential increase of the computational burden if the prediction horizon (N) is longer than 1 and in the case of FCS-MPC is the number of switching states to be studied (J) is high. This fact was critical in the past but nowadays the high-speed microprocessors can carry out complex iterative calculations and the FCS-MPC methods can be executed with sampling times around several decades of microseconds [44]. Besides, MPC techniques like GPC can deal with long prediction horizons without increasing significantly the computational burden [12]. In addition, some authors have developed FCS-MPC techniques that evaluate a reduced set of switching states in cases where the possible switching states are high. For instance, in [34] a three-phase cascaded H-bridge multilevel converter has been considered with $N = 1$. This converter has

125 possible voltage vectors, but the proposed method just calculates the cost function for the 7 vectors located around the last voltage vector applied to the converter. In spite of this, finding computational efficient MPC control algorithms is an open issue.

Usually considered an advantage, the FCS-MPC method avoids using a modulation stage. However, this usually leads to spread harmonic spectra of the output waveforms. This can be solved taking it into account in the cost function [45] or using a modulation stage and applying the FCS-MPC considering all the possible combinations of the switching states of the converter [46].

Another MPC concern is about the design of an efficient cost function and the tuning of the weighting factors. In this case, it can be affirmed that a systematic way to design the cost function with the best weighting factors tuning is still missing. However, some works have introduced a first approach to solve the problem facilitating the electrical engineers design work [47].

Finally, it should be noticed that there is a lack of analytical tools to evaluate performance of MPC for power converters and drives without having to carry out extensive simulations or experiments. Therefore, it is expected that another area of future research would be the development of such tools.

VIII. Conclusions

Model predictive control is a well-known technique to achieve a high performance operation in a wide applications range. Since decades it has been successfully applied to chemical processes with low sampling requirements. However, in the last decade the academia has demonstrated that MPC can be applied to control other systems such as electrical machines and drives. Critical challenges as the accuracy of the models, high sampling rates and high computational cost have been overcome due to continuous evolution of the microprocessors technology and the effort of the researchers. The last step of the MPC to become mature is currently being done and some companies have been attracted by this control method. Hopefully just one step ahead, the MPC will be extensively applied to control complex electrical systems.

Acknowledgment

The authors gratefully acknowledge the financial support provided by the Andalusian Government and the European Commission (ERDF) under the project P11-TIC-7070 and the Ministerio de Economia y Competitividad of the Spanish Government and the European Commission (ERDF) under the project ENE2012-36897.

References

[1] J. H. Lee, "Model Predictive Control: Review of the Three Decades of Development," *International Journal of Control, Automation, and Systems*, vol. 9, no. 3, pp. 415–424, 2011.

[2] M. Morari and J. H. Lee, "Model predictive control: past, present and future," *Computers and Chemical Engineering*, vol. 23, pp. 667–682, 1999.

[3] S. Kouro, P. Cortes, R. Vargas, U. Ammann, and J. Rodriguez, "Model Predictive Control—A Simple and Powerful Method to Control Power Converters," *IEEE Transactions on Industrial Electronics*, vol. 56, no. 6, pp. 1826–1838, 2009.

[4] A. Linder, R. Kanchan, R. Kennel, and P. Stolze, *Model-Based Predictive Control of Electric Drives*. Cuvillier Verlag Göttingen, 2010.

[5] J. Rodriguez and P. Cortes, *Predictive control of power converters and electrical drives*, 1st ed. Wiley-IEEE Press, 2012.

[6] J. Rodriguez, M. P. Kazmierkowski, J. R. Espinoza, P. Zanchetta, H. Abu-Rub, H. A. Young, and C. A. Rojas, "State of the Art of Finite Control Set Model Predictive Control in Power Electronics," *IEEE Transactions on Industrial Informatics*, vol. 9, no. 2, pp. 1003–1016, May 2013.

[7] http://ieeexplore.ieee.org/xplore/home.jsp. [Online]. Available: http://ieeexplore.ieee.org/Xplore/home.jsp

[8] E. F. Camacho and C. Bordons, *Model Predictive Control*. NewYork: Springer-Verlag, 1999.

[9] P. Cortes, M. P. Kazmierkowski, R. M. Kennel, D. E. Quevedo, and J. Rodriguez, "Predictive control in power electronics and drives," *Industrial Electronics, IEEE Transactions on*, vol. 55, no. 12, pp. 4312–4324, 2008.

[10] S. Mariethoz and M. Morari, "Explicit model-predictive control of a pwm inverter with an lcl filter," *Industrial Electronics, IEEE Transactions on*, vol. 56, no. 2, pp. 389–399, 2009.

[11] D. W. Clarke, C. Mohtadi, and P. S. Tuffs, "Generalized predictive controlpart i. the basic algorithm," *Automatica*, vol. 23, no. 2, pp. 137–148, Mar. 1987. [Online]. Available: http://dx.doi.org/10.1016/0005-1098(87)90087-2

[12] S. Vazquez, C. Montero, C. Bordons, and L. G. Franquelo, "Model predictive control of a vsi with long prediction horizon," in *Industrial Electronics (ISIE), 2011 IEEE International Symposium on*, 2011, pp. 1805–1810.

[13] P. Cortes, J. Rodriguez, C. Silva, and A. Flores, "Delay Compensation in Model Predictive Current Control of a Three-Phase Inverter," *IEEE Transactions on Industrial Electronics*, vol. 59, no. 2, pp. 1323–1325, 2012.

[14] D. E. Quevedo, R. P. Aguilera, M. A. Perez, P. Cortes, and R. Lizana, "Model predictive control of an afe rectifier with dynamic references," *Power Electronics, IEEE Transactions on*, vol. 27, no. 7, pp. 3128–3136, 2012.

[15] J. M. Carrasco, L. G. Franquelo, J. T. Bialasiewicz, E. Galvan, R. C. P. Guisado, M. A. M. Prats, J. I. Leon, and N. Moreno-Alfonso, "Power-electronic systems for the grid integration of renewable energy sources: A survey," *Industrial Electronics, IEEE Transactions on*, vol. 53, no. 4, pp. 1002–1016, 2006.

[16] S. Vazquez, S. M. Lukic, E. Galvan, L. G. Franquelo, and J. M. Carrasco, "Energy storage systems for transport and grid applications," *Industrial Electronics, IEEE Transactions on*, vol. 57, no. 12, pp. 3881–3895, 2010.

[17] J. Dixon, L. Moran, J. Rodriguez, and R. Domke, "Reactive power compensation technologies: State-of-the-art review," *Proceedings of the IEEE*, vol. 93, no. 12, pp. 2144–2164, 2005.

[18] S. Vazquez, J. A. Sanchez, J. M. Carrasco, J. I. Leon, and E. Galvan, "A model-based direct power control for three-phase power converters," *Industrial Electronics, IEEE Transactions on*, vol. 55, no. 4, pp. 1647–1657, 2008.

[19] M. Reyes, P. Rodriguez, S. Vazquez, A. Luna, R. Teodorescu, and J. M. Carrasco, "Enhanced decoupled double synchronous reference frame current controller for unbalanced grid-voltage conditions," *Power Electronics, IEEE Transactions on*, vol. 27, no. 9, pp. 3934–3943, 2012.

[20] P. Cortes, J. Rodriguez, P. Antoniewicz, and M. Kazmierkowski, "Direct power control of an afe using predictive control," *Power Electronics, IEEE Transactions on*, vol. 23, no. 5, pp. 2516–2523, 2008.

[21] S. A. Larrinaga, M. A. R. Vidal, E. Oyarbide, and J. R. T. Apraiz, "Predictive control strategy for dc/ac converters based on direct power control," *Industrial Electronics, IEEE Transactions on*, vol. 54, no. 3, pp. 1261–1271, 2007.

[22] R. Aguilera, S. Vazquez, D. Quevedo, and L. G. Franquelo, "Generalized predictive direct power control for ac/dc converters," in *ECCE 2013 - IEEE ECCE Asia Downunder*, 2013.

[23] P. Zanchetta, P. Cortes, M. Perez, J. Rodriguez, and C. Silva, "Finite states model predictive control for shunt active filters," in *IECON 2011 - 37th Annual Conference on IEEE Industrial Electronics Society*, 2011, pp. 581–586.

[24] R. Vargas, J. Rodríguez, U. Ammann, and P. W. Wheeler, "Predictive Current Control of an Induction Machine Fed by a Matrix Converter With Reactive Power Control," *IEEE Transactions on Industrial Electronics*, vol. 55, no. 12, pp. 4362–4371, 2008.

[25] F. Villarroel, J. R. Espinoza, C. A. Rojas, J. Rodriguez, M. Rivera, and D. Sbarbaro, "Multiobjective Switching State Selector for Finite-States Model Predictive Control Based on Fuzzy Decision Making in a Matrix

Converter," *IEEE Transactions on Industrial Electronics*, vol. 60, no. 2, pp. 589–599, Feb. 2013.

[26] M. Rivera, A. Wilson, C. A. Rojas, J. Rodriguez, J. R. Espinoza, P. W. Wheeler, and L. Empringham, "A Comparative Assessment of Model Predictive Current Control and Space Vector Modulation in a Direct Matrix Converter," *IEEE Transactions on Industrial Electronics*, vol. 60, no. 2, pp. 578–588, Feb. 2013.

[27] H. S. Patel and R. G. Hoft, "Generalized techniques of harmonic elimination and voltage control in thyristor inverters: Part i–harmonic elimination," *Industry Applications, IEEE Transactions on*, vol. IA-9, no. 3, pp. 310–317, 1973.

[28] S. Kouro, B. La Rocca, P. Cortes, S. Alepuz, B. Wu, and J. Rodriguez, "Predictive control based selective harmonic elimination with low switching frequency for multilevel converters," in *Energy Conversion Congress and Exposition, 2009. ECCE 2009. IEEE*, 2009, pp. 3130–3136.

[29] E. Jacobsen and R. Lyons, "The sliding dft," *Signal Processing Magazine, IEEE*, vol. 20, no. 2, pp. 74–80, 2003.

[30] L. G. Franquelo, J. Napoles, R. C. P. Guisado, J. I. Leon, and M. A. Aguirre, "A flexible selective harmonic mitigation technique to meet grid codes in three-level pwm converters," *Industrial Electronics, IEEE Transactions on*, vol. 54, no. 6, pp. 3022–3029, 2007.

[31] J. Napoles, J. I. Leon, R. Portillo, L. G. Franquelo, and M. A. Aguirre, "Selective harmonic mitigation technique for high-power converters," *Industrial Electronics, IEEE Transactions on*, vol. 57, no. 7, pp. 2315–2323, 2010.

[32] H. Aggrawal, J. I. Leon, L. G. Franquelo, S. Kouro, P. Garg, and J. Rodriguez, "Model predictive control based selective harmonic mitigation technique for multilevel cascaded h-bridge converters," in *IECON 2011 - 37th Annual Conference on IEEE Industrial Electronics Society*, 2011, pp. 4427–4432.

[33] R. Vargas, P. Cortes, U. Ammann, J. Rodriguez, and J. Pontt, "Predictive control of a three-phase neutral-point-clamped inverter," *Industrial Electronics, IEEE Transactions on*, vol. 54, no. 5, pp. 2697–2705, 2007.

[34] P. Cortes, A. Wilson, S. Kouro, J. Rodriguez, and H. Abu-Rub, "Model predictive control of multilevel cascaded h-bridge inverters," *Industrial Electronics, IEEE Transactions on*, vol. 57, no. 8, pp. 2691–2699, 2010.

[35] P. Lezana, R. Aguilera, and D. E. Quevedo, "Model predictive control of an asymmetric flying capacitor converter," *Industrial Electronics, IEEE Transactions on*, vol. 56, no. 6, pp. 1839–1846, 2009.

[36] A. Kulka, T. Undeland, S. Vazquez, and L. G. Franquelo, "Stationary frame voltage harmonic controller for standalone power generation," in *Power Electronics and Applications, 2007 European Conference on*, 2007, pp. 1–10.

[37] P. Cortes, G. Ortiz, J. I. Yuz, J. Rodriguez, S. Vazquez, and L. G. Franquelo, "Model predictive control of an inverter with output lc filter for ups applications," *Industrial Electronics, IEEE Transactions on*, vol. 56, no. 6, pp. 1875–1883, 2009.

[38] P. Cortes, J. Rodriguez, S. Vazquez, and L. G. Franquelo, "Predictive control of a three-phase ups inverter using two steps prediction horizon," in *Industrial Technology (ICIT), 2010 IEEE International Conference on*, 2010, pp. 1283–1288.

[39] M. P. Kazmierkowski, L. G. Franquelo, J. Rodriguez, M. Perez, and J. I. Leon, "High-performance motor drives," *Industrial Electronics Magazine, IEEE*, vol. 5, no. 3, pp. 6–26, 2011.

[40] H. Miranda, P. Cortes, J. I. Yuz, and J. Rodriguez, "Predictive Torque Control of Induction Machines Based on State-Space Models," *IEEE Transactions on Industrial Electronics*, vol. 56, no. 6, pp. 1916–1924, 2009.

[41] S. Qin and T. Badgwell, "A survey of industrial model predictive control technology," *Control Engineering Practice*, vol. 11, no. 7, pp. 733–764, Jul. 2003. [Online]. Available: http://dx.doi.org/10.1016/s0967-0661(02)00186-7

[42] C. Xia, M. Wang, Z. Song, and T. Liu, "Robust model predictive current control of three-phase voltage source pwm rectifier with online disturbance observation," *Industrial Informatics, IEEE Transactions on*, vol. 8, no. 3, pp. 459–471, 2012.

[43] Z. Song, C. Xia, and T. Liu, "Predictive current control of three-phase grid-connected converters with constant switching frequency for wind energy systems," *Industrial Electronics, IEEE Transactions on*, vol. 60, no. 6, pp. 2451–2464, 2013.

[44] R. K. Cavin, P. Lugli, and V. V. Zhirnov, "Science and engineering beyond moore's law," *Proceedings of the IEEE*, vol. 100, no. Special Centennial Issue, pp. 1720–1749, 2012.

[45] P. Cortes, J. Rodriguez, D. E. Quevedo, and C. Silva, "Predictive current control strategy with imposed load current spectrum," *Power Electronics, IEEE Transactions on*, vol. 23, no. 2, pp. 612–618, 2008.

[46] S. Vazquez, J. I. Leon, L. G. Franquelo, J. M. Carrasco, O. Martinez, J. Rodriguez, P. Cortes, and S. Kouro, "Model predictive control with constant switching frequency using a discrete space vector modulation with virtual state vectors," in *Industrial Technology, 2009. ICIT 2009. IEEE International Conference on*, 2009, pp. 1–6.

[47] P. Cortes, S. Kouro, B. La Rocca, R. Vargas, J. Rodriguez, J. I. Leon, S. Vazquez, and L. G. Franquelo, "Guidelines for weighting factors design in model predictive control of power converters and drives," in *Industrial Technology, 2009. ICIT 2009. IEEE International Conference on*, 2009, pp. 1–7.